Accepted Manuscript

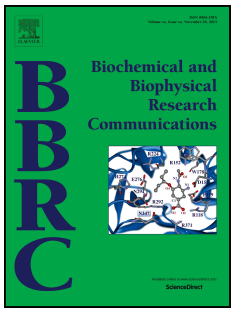

Structural basis of the substrate recognition of hydrazidase isolated from *Microbacterium* sp. strain HM58-2, which catalyzes acylhydrazide compounds as its sole carbon source

Tomonori Akiyama, Misaki Ishii, Atsushi Takuwa, Ken-Ichi Oinuma, Yasuyuki Sasaki, Naoki Takaya, Shunsuke Yajima

PII: S0006-291X(16)32022-8

DOI: 10.1016/j.bbrc.2016.11.148

Reference: YBBRC 36852

To appear in: *Biochemical and Biophysical Research Communications*

Received Date: 20 November 2016

Accepted Date: 27 November 2016

Please cite this article as: T. Akiyama, M. Ishii, A. Takuwa, K.-I. Oinuma, Y. Sasaki, N. Takaya, S. Yajima, Structural basis of the substrate recognition of hydrazidase isolated from *Microbacterium* sp. strain HM58-2, which catalyzes acylhydrazide compounds as its sole carbon source, *Biochemical and Biophysical Research Communications* (2016), doi: 10.1016/j.bbrc.2016.11.148.

Structural basis of the substrate recognition of hydrazidase isolated from *Microbacterium* sp. strain HM58-2, which catalyzes acylhydrazide compounds as its sole carbon source

Tomonori Akiyama[a], Misaki Ishii[a], Atsushi Takuwa[b], Ken-Ichi Oinuma[b], Yasuyuki Sasaki[a], Naoki Takaya[b], Shunsuke Yajima[a]*

[a]Department of Bioscience, Tokyo University of Agriculture, Setagaya-ku, Tokyo 156-8502, Japan

[b]Faculty of Life and Environmental Sciences, University of Tsukuba, Tennodai, Tsukuba 305-8572 Japan

*Corresponding author

E-mail address: yshun@nodai.ac.jp (S. Yajima).

Keywords: amidase signature family; *Microbacterium*; protein structure; substrate specificity; X-ray crystallography

Abstract

Hydrazidase was an enzyme that remained unidentified for a half century. However, recently, it was purified, and its encoding gene was cloned. *Microbacterium* sp. strain HM58-2 grows with acylhydrazides as its sole carbon source; it produces hydrazidase and degrades acylhydrazides to acetate and hydrazides. The bacterial hydrazidase belongs to the amidase signature enzyme family and contains a Ser-cisSer-Lys catalytic motif. The condensation of hydrazine and carbonic acid produces various hydrazides, some of which are raw materials for synthesizing pharmaceuticals and other useful chemicals. Although natural hydrazide compounds have been identified, the metabolic systems for hydrazides are not fully understood. Here, we report the crystal structure of hydrazidase from *Microbacterium* sp. strain HM58-2. The active site was revealed to consist of a Ser-cisSer-Lys catalytic triad, in which Ser179 forms a covalent bond with a carbonyl carbon of the substrate. 4-Hydroxybenzoic acid hydrazide bound to the S179A mutant, showing an oxyanion hole composed of the three backbone amide groups. Furthermore, H336 in the non-conserved region in the amidase family may define the substrate specificity, which was confirmed by mutation analysis. A wild-type apoenzyme structure

revealed an unidentified molecule covalently bound to S179, representing a tetrahedral intermediate.

1. Introduction

Hydrazine and its derivatives are important compounds for various applications such as pharmaceuticals, dyes, and herbicide synthesis. Acylated derivatives of hydrazine are described as $R_1R_2N\text{-}N(R_3)C(=O)R_4$ and are called (acyl)hydrazides. An antituberculosis agent, isonicotinic acid hydrazide, known as isoniazid (1) is a well-known hydrazide. Isocarboxazid is used as an antidepressant (2), and other hydrazides are used as agricultural herbicides, pesticides, insecticides, fungicides, and plant growth regulators (3). In industry, hydrazides are applicable to cross-linking acrylic emulsions, curing epoxy resins, and scavenging formaldehyde through their powerful reactivity with ketone and epoxy groups (4).

Natural compounds possessing a hydrazide moiety have been also identified (5). Agaritine from the commercial mushroom *Agaricus bisporus* and its relatives were the first natural hydrazides to be discovered (6). A hydrazide degrading enzyme, with hydrazide hydrolyzing activity, was discovered in *Mycobacterium avium* that could hydrolyze various hydrazides, including isonicotinic acid hydrazide. It was named hydrazidase (7). However,

the molecular identification of this enzyme had not been pursued.

Recently, we isolated *Microbacterium* sp. strain HM58-2 from soil; this strain grows with an acylhydrazide such as 4-hydroxybenzoic acid 1-phenylethylidene hydrazide (HBPH) as its sole carbon source, and we cloned the hydrazidase gene responsible for the reaction (8). Hydrazidase hydrolyzes HBPH to 4-hydroxy benzoic acid and acetophenone hydrazone (Fig. 1A). The amino acid sequence of the hydrazidase shares an amidase signature with a Ser-Ser-Lys motif. The amidase signature enzyme family contains a signature region of approximately 130 amino acids that includes a canonical catalytic triad and Gly/Ser-rich motif (GGSS[GS]G) (9). The enzymes in this family exhibit a variety of functions, such as peptide amidase (PAM), glutamyl-tRNA amidotransferase subunit A (GatA), indole-acetamide hydrolase (IAAH), eukaryotic amidase group 1 (E1), eukaryotic amidase group 2 (E2), and 6-aminohexanoate-cyclic-dimer hydrolase (AH) (10). The amino acid sequence of hydrazidase shares homology with those of GatA and fatty acid amide hydrolase (FAAH) (8), whose substrates are different from hydrazidase. To elucidate the substrate recognition mechanism of hydrazidase, we determined the crystal structures of hydrazidase for the wild-type and the mutant complexed with a hydrazide compound.

These structures revealed critical residues for the catalytic reaction and substrate binding in hydrazidase.

2. Materials and Methods

2.1. Protein expression and purification

The hydrazidase gene was cloned into pET28a(+), and the recombinant protein was expressed in *Escherichia coli* BL21(DE3), as described previously (8). The *E. coli* strain harboring hydrazidase was cultured in LB media with 25 μg/mL kanamycin at 37°C. The protein was induced by isopropyl-thio-β-galactopyranoside, and then, the culture was continued for 6 hr at 30°C. The supernatant from the cell lysate was loaded on a Ni-NTA agarose column. The column was washed with buffer A [20 mM Tris-HCl, pH 7.5, 100 mM NaCl, 20 mM imidazole, 10% glycerol], and then, the recombinant protein was eluted with buffer B [20 mM Tris-HCl, pH 7.5, 100 mM NaCl, 500 mM imidazole, 10% glycerol]. The eluted protein was dialyzed with buffer C [20 mM Tris-HCl, pH 7.5] followed by purification with a MonoQ column. The collected fraction was further purified with a HiLoad 16/60 column with buffer E [20 mM Tris-HCl, pH 7.5, 10% glycerol]. Hydrazidase

was concentrated to 20 mg/mL with an Amicon Ultra 30K cartridge for crystallization.

2.2. Crystallization and structure determination

Crystals were grown at 4°C by the hanging-drop vapor-diffusion method in a drop consisting of 1.0 μl of protein solution and 1.0 μl of a crystallization reservoir solution containing 0.1 M imidazole, 0.17 M $LiSO_4$, and 2 M $(NH_4)_2SO_4$. Under these conditions, two crystal forms were obtained, that for wild-type hydrazidase belongs to the space group $C222_1$ with a = 122.1 Å, b = 127.9 Å, c = 158.8 Å, and $\alpha = \beta = \gamma = 90°$, and that for the S197A mutant belongs to the space group $P2_1$ with unit cell parameters a = 73.0 Å, b = 126.5 Å, c = 123.2 Å, $\alpha = 90°$, $\beta = 105.7°$, and $\gamma = 90°$. Prior to data collection, the crystal was transferred instantly into a cryoprotectant solution [21%(w/v) xylitol in the reservoir solution] and flash-cooled in a liquid-nitrogen gas stream at 95 K. Diffraction data were collected on beamline AR BL-NW12A equipped with a Quantum 210 CCD detector or BL-17A with a Quantum 270 detector (Area Detector Systems Corp., CA) at the Photon Factory, High Energy Accelerator Research Organization, Tsukuba, Japan. The diffraction data were processed using the HKL2000 package (11).

The initial structure of wild-type hydrazidase was solved by molecular replacement using MoRDa (12) followed by automated model building by Arp/wArp (13). The iterative model refinement was carried out using Coot (14) and REFMAC5 (15). The initial structure of the S179A mutant was solved by the molecular replacement method using MORLEP (16) in the CCP4 suite (17) with the wild-type structure as a search model. Data collection and refinement statistics are presented in Table 1.

To elucidate the structure of the hydrazidase-substrate complex, crystals were soaked instantly with 3 mM 4-hydroxybenzoic acid hydrazide (HBH) (Sigma-Aldrich Co. LLC. MO) in the cryoprotectant solution. All figures of protein structures were generated using PyMOL (v.1.4.1; Schrödinger). The atomic coordinates and structure factors for the wild-type and the S197A mutant have been deposited in the Protein Data Bank under accession codes 5H6T and 5H6S, respectively.

2.3. Mutant preparation and enzyme assay

The plasmid pET-hydrazidase was mutagenized for single amino acid substitutions of C129A, C129S, and H336A of hydrazidase using a PrimeSTAR Mutagenesis Basal Kit

(TaKaRa Bio Inc.) according to the manufacturer's instructions with each set of the following primers: C129A: forward 5′-GACCTGGCCATCCGATGGAACTCCGTG-3′ and reverse 5′-TCGGATGGCCAGGTCGGGGATTCCCGC-3′, C129S: forward 5′-GACCTGTCCATCCGATGGAACTCCGTG-3′ and reverse 5′-TCGGATGGACAGGTCGGGGATTCCCGC-3′, and H336A: forward 5′-CGGATGGCCATCGTGGACATGTTCGGC-3′ and reverse 5′-CACGATGGCCATCCGCTCGCTGGCGAT-3′. Purified mutants were subjected to the enzyme assay. Reaction mixtures contained 20 mM Tris-HCl, pH 7.5, 0.2 mM HBH, and 5%(v/v) dimethyl sulfoxide in a total volume of 200 μL. The enzyme was added, and the reaction proceeded at 30°C for 60 min before being stopped by adding 200 μL of ice-cold acetonitrile. The reaction product, 4-hydroxybenzoic acid, was measured using a high-performance liquid chromatography (HPLC) system equipped with an ODS-4 column (4.6 by 250 mm) by monitoring the absorption at 250 nm. The mobile-phase solvent system contained 50 mM Tris-HCl (pH 7.5) and acetonitrile (6:4(v/v)).

3. Results and Discussion

3.1. Overall structure of hydrazidase

Crystals of the wild-type and the S179A mutant of hydrazidase were obtained in different space groups, which belong to $C222_1$ and $P2_1$, respectively, in an identical reservoir [0.1 M imidazole, pH 8.3, 0.17 M $LiSO_4$, 2 M $(NH_4)_2SO_4$]. These crystal structures were refined at a 1.6 Å- and 1.8 Å-resolution, respectively. Both the wild-type and mutant hydrazidase were composed of a homodimer structure (Fig. 1C) and one dimer and two dimers in an asymmetric unit of $C222_1$ and $P2_1$ crystals, respectively. In the $C222_1$ structure, the electron density for the His x 6 tag sequence at the N-terminus was clearly observed in one subunit of the dimer, which contributed to a crystal contact. MoRDa software used for the molecular replacement method selected the coordinates of the PDB code 3H0L for glutamyl-tRNA amidotransferase subunit A (GatA) (18) as a search model. 3D structure comparison using the Dali server (19) also revealed a top hit of GatA (PDB code: 2GI3) (Z-score = 48.8, rmsd = 2.1 Å) followed by aryl acylamidase (PDB code: 4YJ6) (Z-score = 48.7, rmsd = 2.9 Å) (20) and a series of GatA proteins including 3H0L. Then, rat fatty acid amino hydrolase (FAAH) (PDB code: 1MT5) (21) and *Granulibacter bethesdensis* allophanate hydrolase (PDB code: 4GYS) (22) were also listed. Superposing the structures

of the hydrazidase and the amidases listed by the Dali server revealed that most of their overall structures fit well except for two regions around the entrances of the substrate binding pocket (Fig. 2A, B, C). Amino acid sequence alignment of these amidases showed that those two regions (N203-E215 and E311-D349) are located at the C-terminus of the amidase signature and are not conserved (Fig. 2D). The amino-acid differences may cause structural varieties and hence alter the substrate specificity of these enzymes. The average b-factors of the whole hydrazidase chains A and B (wild-type) were 14.1 and 15.5, respectively, whereas those of region G206-N211 were higher (32.9 and 30.8 for chains A and B, respectively). These results agree with the flexible property of the entrance that enables it to open/close upon binding the substrate.

3.2. Substrate binding

The amidase signature enzyme family contains three highly conserved residues characterized by the Ser-cisSer-Lys catalytic triad. The amino acid sequence alignment (8) as well as the crystal structure of the wild-type hydrazidase identified S179-cisS155-K80 as the catalytic triad. To elucidate the substrate binding mode, we solved the crystal structure

of the S179A mutant complexed with 4-hydroxybenzoic acid hydrazide (HBH) (Fig. 1B). As shown in Figures 3A and 3B, HBH bound to the catalytic site with the carbonyl oxygen formed three hydrogen bonds with the backbone amide groups of L176, G177, and S179A. This coordination of the carbonyl oxygen binding represented the oxyanion hole formed by these three amide groups, which is important to stabilize the tetrahedral transition states in the reaction.

The 4-hydroxy oxygen of HBH formed a hydrogen bond with a water molecule, which connected to H336 by another hydrogen bond. This binding was used to determine the substrate specificity of the hydrazidase because H336 positions in a structurally non-conserved region among the proteins described in the previous section (Fig. 2D). The same binding mode using the water molecule and H336 was also observed in the wild-type (see below). Another hydrogen bond was formed between a carbonyl oxygen of C129 and the amide group of HBH (Fig. 3B). Hydrazidase hydrolyzes HBH more effectively than 4-hydroxybenzamide (HBA) (8). The only difference between these two compounds is the additional amide group in HBH next to the amide nitrogen in HBA. Without this amide group, the hydrogen bond is lost between C129 and HBA, which is expected to result in

weak binding to HBA. The potential roles of the H336 and C129 residues in substrate binding were investigated by analyzing the enzyme activities of the C129A, C129S, and H336A mutants. The catalytic activity of the H336A mutant was markedly reduced to 1% (Fig. 3E). Therefore, H336 is considered to be an important residue in determining substrate specificity. The activities of C129A and C129S also decreased to 10% and 30%, respectively, relative to that of the wild-type (Fig. 3E). These mutations may induce some conformational change at the respective positions because HBH binds to C129 via a backbone carbonyl oxygen.

When the structures of the wild-type and S179A mutant were superposed, the side chains of the residues in the substrate binding site of both structures fit very well (Fig. 3D). The distance between the OG atom of S179 in the wild-type and the carbonyl carbon of HBH in the mutant structure was 1.7 Å (Fig. 3B). Therefore, in combination with the three hydrogen bonds for the oxyanion hole, the bound position of HBH is considered to reflect the catalytic site of hydrazidase.

HBPH, which is an effective substrate for hydrazidase, also has an imide group at the same position as the amide of HBH. When we manually superposed HBPH with HBH using the

4-hydroxybenzene ring, the acetophenone portion hydrophobically interacted mainly with the residues L128 and Ile130 (Supplementary Fig. 1). This could lead to more a stable binding of HBPH than in the case of HBH.

3.3. The catalytic site of the wild-type hydrazidase

At the catalytic site of the wild-type hydrazidase, a clear electron density was observed. The shape of the density indicates that a cyclic compound bound covalently to the S179 residue. Attempts to fit various compounds originated from the protein solution, reservoir solution, and cryoprotectant to the density did not identify any molecule. We, therefore, attempted to fit a dummy molecule. Based on the shape of the electron density, 1,4-dimethyl cyclohexane was initially chosen to be fit. Then, based on the distances between the atoms of the molecule and surrounding residues, some atoms were replaced with oxygen atoms to make hydrogen bonds, resulting in 2,5-dihydroxy 1,3-dioxan. It is also possible that some of them could be nitrogen atoms. This dummy molecule was fit to the density (Fig. 4), and the resulting model indicated that the molecule forms hydrogen bonds with the backbone amide group of G177, a carbonyl oxygen of C129, and the

carbonyl oxygen and amide group of S155 and H336 by way of a water molecule (Fig. 3C). The distance between the OG atom of S179 and the carbon atom of the dummy molecule was 1.5 Å, which is consistent with the covalent binding of the molecule to S179 and represents a tetrahedral conformation generated by nucleophilic attack of the side chain of S179 to the substrate carbonyl carbon, as seen in the proteins in the amidase signature enzyme family (9). The hydrazidase used in this study hydrolyses an artificial synthetic substrate HBPH, and no natural substrate for the enzyme has been identified. This unknown compound may be a candidate, but further study is needed.

Acknowledgments

This project was supported by JSPS KAKENHI Grant Number 15K07369 to S.Y. and partially supported by the Platform Project for Supporting in Drug Discovery and Life Science Research (Platform for Drug Discovery, Informatics, and Structural Life Science) from the Japan Agency for Medical Research and Development (AMED). We thank the beamline staff at Photon Factory for the technical support during data collection.

References

[1] T. Scior, I. Meneses Morales, S.J. Garces Eisele, D. Domeyer, S. Laufer, Antitubercular isoniazide and drug resistance of *Mycobacterium tuberculosis*-a review, Arch. Pharm. (Weinheim) 335 (2002) 511-525.

[2] F. López-Muñoz, C. Alamo, G. Juckel, H.J. Assion, Half a century of antidepressant drugs: on the clinical introduction of monoamine oxidase inhibitors, tricyclics, and tetracyclics. Part I: Monoamine oxidase inhibiotrs, J. Clin. Psychopharmacol. 27 (2007) 555-559.

[3] B. Toth, A review of the natural occurrence, synthetic production and use of carcinogenic hydrazines and related chemicals, In Vivo 14 (2000) 299-319.

[4] H.W. Schiessl, Hydrazine and its derivatives, in: A. Seidel, M. Bickford (Eds.), Kirk-Othmer encyclopedia of chemical technology, vol 13. John Wiley and Sons, Inc., New Jersey. 2000, pp. 562-607.

[5] L.M. Blair, J. Sperry, Natural products containing a nitrogen-nitrogen bond, J. Nat. Prod. 76 (2013) 794-812.

[6] B. Levenberg, Structure and enzymatic cleavage of agaritine, a phenylhydrazide of L-glutamic acid isolated from *Agaricaceae*. J. Am. Chem. Soc. 83 (1961) 503-504.

[7] I. Toida, Isoniazid-hydrolyzing enzyme of mycobacteria, Am. Rev. Respir. Dis. 85 (1962) 720-726.

[8] K. Oinuma, A. Takuwa, K. Taniyma, Y. Doi, N. Takaya, Hydrazidase, a novel amidase signature enzyme that hydrolyzes acylhydrazides, J. Bacteriol. 197 (2015) 1115-1124.

[9] S. Shin, T.H. Lee, N.C. Ha, H.M. Koo, S.Y. Kim, H.S. Lee, Y.S. Kim, B.H. Oh, Structure of maonamidase E2 reveals a novel Ser-cisSer-LLys catalytic triad in a new serine hydrolase fold hat is prevalent in nature, Embo J. 21 (2002) 2509-2516.

[10] H.J. Ko, E.W. Lee, W.G. Bang, C.K. Lee, K.H. Kim, I.G. Choi, Molecular characterization of a novel bacterial aryl acylamidase belonging to the amidase signature enzyme family, Mol. Cells 29 (2010) 485-492.

[11] Z. Otwinowski, W. Minor, Processing of X-ray diffraction data collected in oscillation mode, Methods Enzymol. 276 part A (1997) 307-326.

[12] A. Vagin, A. Lebedev, MoRDa – Automatic Molecular Replacement Pipeline, http://www.biomexsolutions.co.uk/morda/

[13] G. Langer, S.X. Gohen, V.S. Lamzin, A. Perrakis, Automated macromolecular model building for X-ray crystallography using ARP/wARP version 7. Nat. Protoc. 3 (2008) 1171-1179.

[14] P. Emsley, B. Lohkamp, W.G. Scott, K. Cowtan, Features and development of Coot,

Acta Crystallogr. D Biol. Crystallogr. 66 (2010) 486-501.

[15] G.N. Murshudov, P. Skubák, A.A. Lebedev, N.S. Pannu, R.A. Steiner, R.A. Nicholls, M.D. Winn, F. Long, A.A. Vagin, REFMAC5 for the refinement of macromolecular crystal structures, Acta Crystallogr. D Biol. Crystallogr. 67 (2011) 355-367.

[16] A. Vagin, A. Teplyakov, MOLREP: an automated program for molecular replacement, J. Appl. Crystallogr. 30 (1997) 1022-1025.

[17] M.D. Winn, C.C. Ballard, K.D. Cowtan, E.J. Dodson, P. Emsley, P.R. Evans, R.M. Keegan, E.B. Krissinel, A.G.W. Leslie, A. McCoy, S.J. McNicholas, , G.N. Murshudov, N.S. Pannu, E.A. Potterton, H.R. Powell, R.J. Read, A. Vagin, K.S. Wilson, Overview of the CCP4 suite and current developments, Acta Crystallogr. D Biol. Crystallogr. 67 (2011) 235-242.

[18] J. Wu, W. Bu, K. Sheppard, M. Kitabatake, S.T. Kwon, D. Söll, J.L. Smith, Insights

into tRNA-dependent amidotransferase evolution and catalysis from the structure of the Aquifex aeolicus enzyme, J. Mol. Biol. 391 (2009) 703-716.

[19] L. Holm, P. Rosenstörm, Dali server: conservation mapping in 3D, Nucleic Acids Res. 38 (2010) W545-W549.

[20] S. Lee, E.H. Park, H.J. Ko, W.G. Bang, H.Y. Kim, I.G. Choi, Crystal structure analysis of a bacterial ary acylamidase belonging to the amidase signature enzyme family, Biochem. Biophys. Res. Commun. 467 (2015) 268-274.

[21] M.H. Bracey, M.A. Hanson, K.R. Masuda, R.C. Stevens, B.F. Cravatt, Structural adaptations in a membrane enzyme that terminates endocannabinoid signaling, Science 298 (2002) 1793-1796.

[22] Y. Lin, M. St Maurice, The structure of allophanate hydrolase from *Granulibacter bethesdensis* provides insights into substrate specificity in the amidase signature family,

Biochemistry 52 (2013) 690-700.

[23] E.F. Pettersen, T.D. Goddard, C.C. Huang, G.S. Couch, D.M. Greenblatt, E.C. Meng, T.E. Ferrin, UCSF Chimera-a visualization system for exploratory research and analysis, J. Comput. Chem. 25 (2004) 1605-1612.

[24] A.T. Brünger, P.D. Adams, G.M. Clore, W.L. DeLano, P.Gros, R.W. Grosse-Kunstleve, J.S. Jiang, J. Kuszewski, M. Nilges, N.S. Pannu, R.J. Read, L.M. Rice, T. Simonson, G.L. Warren, Crystallography & NMR System: A new software suite for macromolecular structure determination, Acta Crystallogr. D Biol. Crystallogr. 54 (1998) 905-921.

Figure legends

Figure 1. Enzymatic reaction and overall structure of hydrazidase from *Microbacterium* sp. strain HM58-2. A. Hydrazidase hydrolyzes HBPH to 4-hydroxy benzoic acid and acetophenone hydrazone. B. The structure of 4-hydroxybenzoic acid hydrazide (HBH). C.

The wild-type hydrazidase ($C222_1$ form) is shown in a cartoon model. The portion colored in pale pink corresponds to the N-terminal His x 6 – tag region. The spheres colored in magenta indicate the catalytic residue S179.

Figure 2. Comparisons of the structures of hydrazidase and other amidases. A-C. The structure of the wild-type hydrazidase is superposed by Chimera (23) with those of the amidases indicated by PDB codes. The colored regions represent structurally non-overlapped regions and correspond to regions 1 and 2 in the sequence alignment in panel D. The green and cyan colors indicate hydrazidase and the indicated amidases, respectively. The spheres colored in magenta and yellow represent HBPH and the residue H336, respectively. D. Sequence alignment of hydrazidase and amidases. Sequence alignment by ClustalW was performed for Hydr (hydrazidase, this study), 2GI3 (GatA), 4GYS (allophanate hydrolase), 4YJ6 (aryl acylamidase), and 1MT5 (FAAH). The black triangles indicate the residues of the catalytic triad. The green and blue triangles indicate the residues C129 and H336, respectively, which formed hydrogen bonds with the substrate. The blue line indicates the conserved amidase signature region, and the orange lines

indicate two regions, which constitute the entrance of the substrate binding pockets.

Figure 3. The catalytic site of hydrazidase. A. Fo-Fc omit map (1.5σ level) of HBH calculated by CNS (24) bound in the catalytic site as in panel B. B. The binding mode of HBH to the catalytic site of the S179A mutant is shown with a stick model. The black dotted lines represent the distances between two atoms that are less than 2.8 Å. The distance between OG of S156 and NE of K80 (a grey dotted line) is 3.3 Å. The cyan colored S179 is from the wild-type when the S179A and the wild-type structures were superposed. The pink dotted line indicates the distance of 1.7 Å. C, A dummy molecule bound to the catalytic site of the wild-type. The black dotted lines represent the distances between two atoms that are less than 3.0 Å, and the pink dotted line indicates a distance of 1.5 Å. D, Superposition of the wild-type and S197A structures. HBPH colored in yellow is also superposed manually based on the position of HBH. E. Catalytic activities of mutant hydrazidases. Catalytic activities of three mutants, C129A, C129S, and H336A, were compared to that of the wild-type as 100%. The procedures for the assay and measurements are described in the Materials and Methods section.

Figure 4. An Fo-Fc omit map of an unknown compound and S179. The map was calculated by omitting the residue S179 using CNS and contoured at 3σ. A dummy molecule colored in cyan is placed in the electron density.

Table 1

Data collection and refinement statistics

Data collection		
	Wild type	S179A+HBH
Beamline	PF-AR BL-NW12A	PF BL-17A
Wavelength (Å)	1.0000	0.9800
Temperature (K)	95	95
Detector	Quantum 210	Quantum 270
Space group	$C222_1$	$P2_1$
Unit cell parameters (Å, °)	a = 122.2, b = 128.1, c = 159.3, $\alpha = \beta = \gamma$ = 90	a = 73.0, b = 126.5, c = 123.2, α = 90, β = 105.7, γ = 90
No. mol in ASU	2	4
Resolution range (Å)	50 – 1.6 (1.63 – 1.6)	50 – 1.8 (1.82 – 1.8)
No. of unique reflections	163385 (8126)	196526 (9687)
Redundancy	6.1 (5.9)	3.8 (3.7)
Completeness (%)	99.9 (100)	97.9 (96.3)
$I/\sigma I$	47.2 (8.9)	29.9 (5.2)
R_{merge}*	0.054 (0.232)	0.065 (0.386)
Refinement		
Resolution range (Å)	34.0 – 1.6 (1.64 – 1.6)	40.6 – 1.8 (1.84 – 1.8)
Completeness (%)	99.7 (98.2)	97.6 (92.6)
No. of reflections	155116 (11835)	186627 (13804)
R_{work}/R_{free}	0.165/0.178 (0.170/0.193)	0.172/0.192 (0.212/0.242)
No. of non-H atoms		
Protein	7055	13788
Water	670	727
Ligand (HBH)†	n.a.	44
R.m.s. deviation		
Bond (Å)	0.008	0.009
Angle (°)	1.429	1.360
Average B factors (Å^2)		

Protein	14.3	17.9
Water	23.5	26.1
Ligand (HBH)[†]	n.a.	25.1
Ramachandran plot		
Favoured (%)	97.2	97.1
Allowed (%)	2.7	2.9
dsiallowed (%)	0.1	0

[*] $R_{merge} = \Sigma_{hkl}\Sigma_i |I_i(hkl) - \langle I(hkl)\rangle| / \Sigma_{hkl}\Sigma_i I_i(hkl)$, where $I_i(hkl)$ is the intensity of an observation and $\langle I(hkl)\rangle$ is the mean value for the unique reflection; summations are over all reflections.

[†]n.a. denotes not applicable.

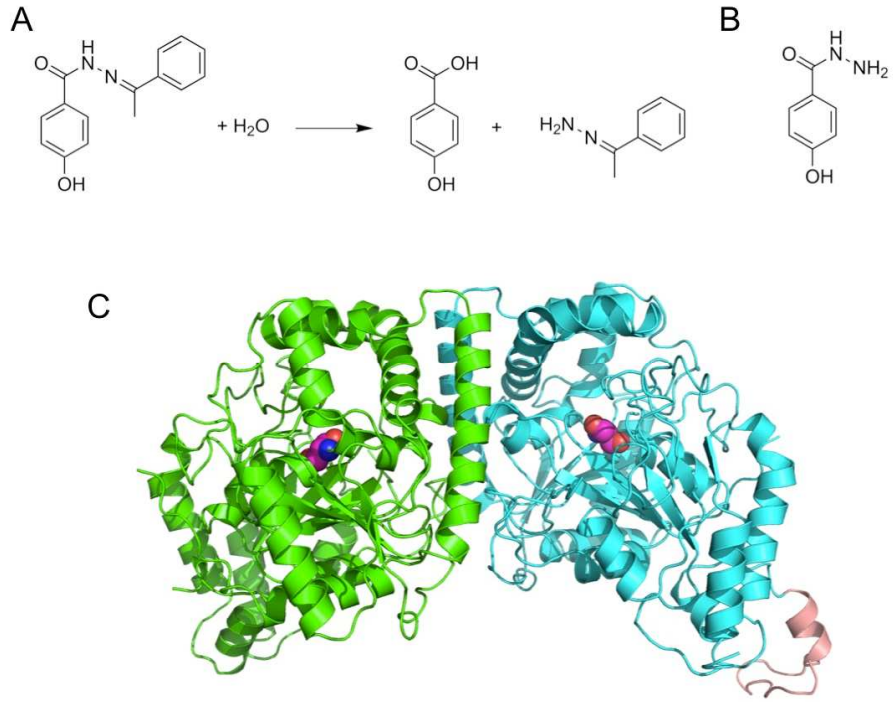

Figure 1

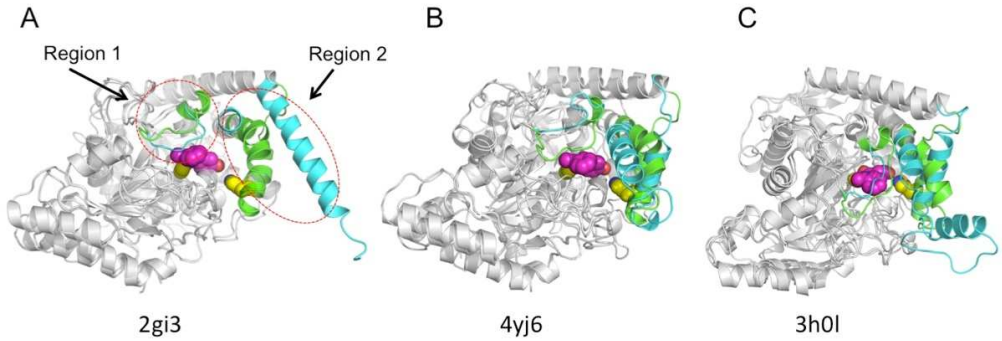

D

```
2GI3  --KGKFWGIPVAIKDNILTLG--MRTTCASRILENYESVFDATVVKKMKEAG--FVVVGKANLDEFAMGSSTERSAFFPT 128
4GYS  -TGKPLYGVPFAVKDNIDVAG--LPCSAACPAFT-YEPDRDATVVARLRAAG--AIVLGKTNLDQFATGLVGTRSPFGAP 135
4YJ6  EPVGMLAGVPTLMKDLFAAKPGWPSTLGGIRALKDARGAAGVWSTYPLKMSGEDSLLLGQTNSPVYGFRGTTDNTFFGPT 150
1MT5  --QGLLYGVPVSLKECFSYKG--HDSTLGLSLNEGMPSESDCVVVQVLKLQG--AVPFVHTNVPQSMLSFDCSNPLFGQT 204
Hydr  TLGGPLDGVPLSIKDSYSVAG--LHRTDGLPVNADVLDAQDDVATARLRAAG--GLVLGHAGIPDLCIRWNSVSGLYGAV 142
                                                                                        
2GI3  RNPWDLERVPGGSSGGSAAAVSAGMVVAALGSDTGGSVRQPASLCGVVGYKPTYGLVSRYG------LVAFASSLDQIGP 202
4GYS  RCVFDQDYISGGSSGSAVAVAAGLVAFSLGTDTAGSGRVPAAFNNLVGVKPTKGLLSTSG------VVPACRSLDCVTV 209
4YJ6  RNPFNLDFNAGGSSGGAAALVADGIVPVAGGTDGGGSIRIPAAWTNTYGFQPSIGRVPFKS----RPNAFHPGPYLYEGP 226
1MT5  MNPWKSSKSPGGSSGGEGALIGSGGSPLGLGTDIGGSIRFPSAFCGICGLKPTGNRLSKSGLKG--CVYGQTAVQLSLGP 282
Hydr  RNPRDLSRTAGGSSGGDAANVAAGFATIGLGGDLGGSIRVPASWCGVYGFRTGPGRIPDANPNGGRSRNVVMELMAQIGP 222
                                                                                        
2GI3  ITKTVRDAAILMEIISGRDENDATTVNRKVDFLSEIEEGVSGMKFAVPEEI-YEHDIEEGVSERFEEALKLLERLGAKVE 281
4GYS  FAASVAEGTLIRRIAEGYDAADPYSRPSQKRRLPHVGLRVG----VPRQDQ-REFYGNTAYAALYQRALDEMISLDAELV 284
4YJ6  ITRTVRDAALAMNVLHGFDRRDPASLRVKLDFTSALAQGVRGKKIGLTLNY-GVFPVQQEIQDLIGKAARVFTELGAHVE 305
1MT5  MARDVESLALCLKALLCEHLFTLDPTVPPLPFREEVYRSSRPLRVGYYETDNYTMPSPAMRRALIETKQRLEAAGHTLIP 362
Hydr  IARSIDDIELAFRIMTGVDRRDTMSSPLG--------------LIEPIEAP-RVAVLRHETGAVLDSSVEEQLDATIEML 287
                                                                                        
2GI3  RVKI-----PHIKYSVATYYVIAPAEASSNLARFDGVKYGLRIKEKGLREMYMKTRNVGFGEEVRRRIMIGTFTLSAAYY 356
4GYS  EIDF-----APFR-DAAKLLYGGPWVAERLEAVGDHLSRAPDSFDPVVRSIVETAKTLSAVDAFRGQYELAALTQQAN-- 356
4YJ6  FVDLGIPYSQKQMSDAWCRMIAIPTVASMQALRKEGIDLYGEHRADIPDALMKWIDAVADISVQQISADQLLRTTVFDCM 385
1MT5  FLPNNIPYALEVLSAGGLFSDGGRSFLQNFKGDFVDPCLGDLILILRLPSWFKRLLSLLLKPLFPRLAAFLNSMRPRSAE 442
Hydr  RAEG-----YVVEENVLPDLHRAPEVWAEIVGTELIHRVLPEVAELVIASERMHIVDMFGAYELGADVGAYLTALEER-- 360
```

Figure 2

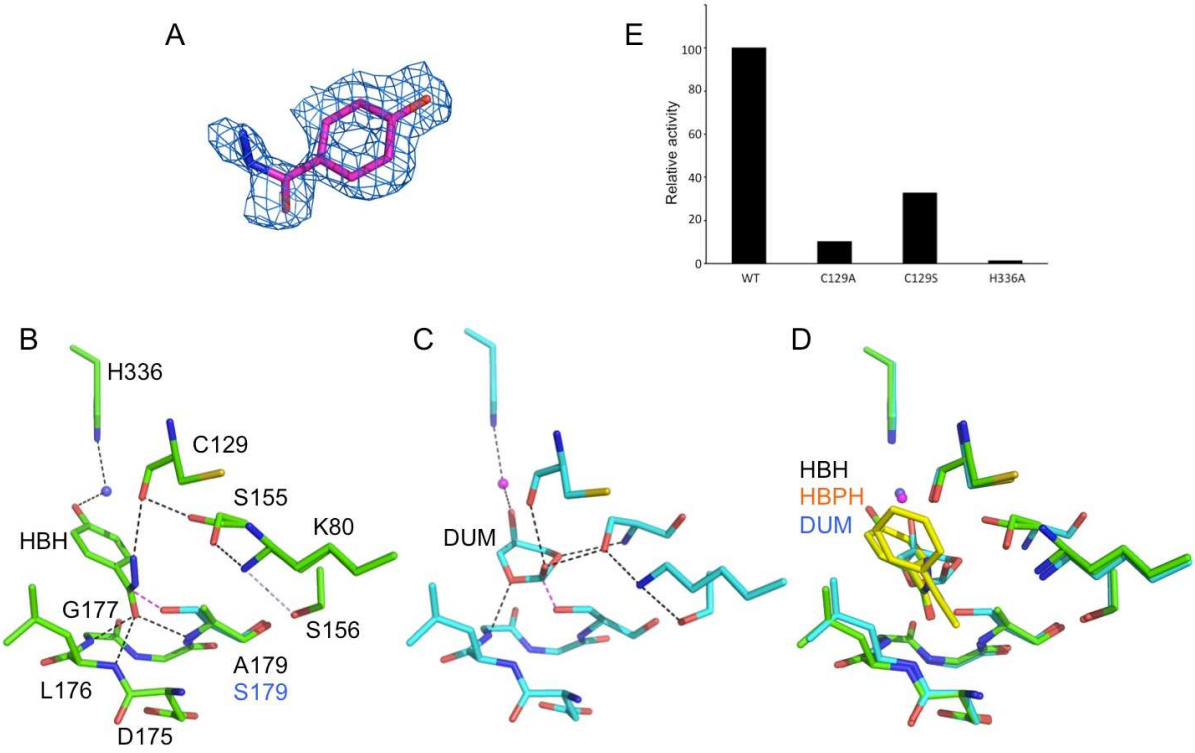

Figure 3

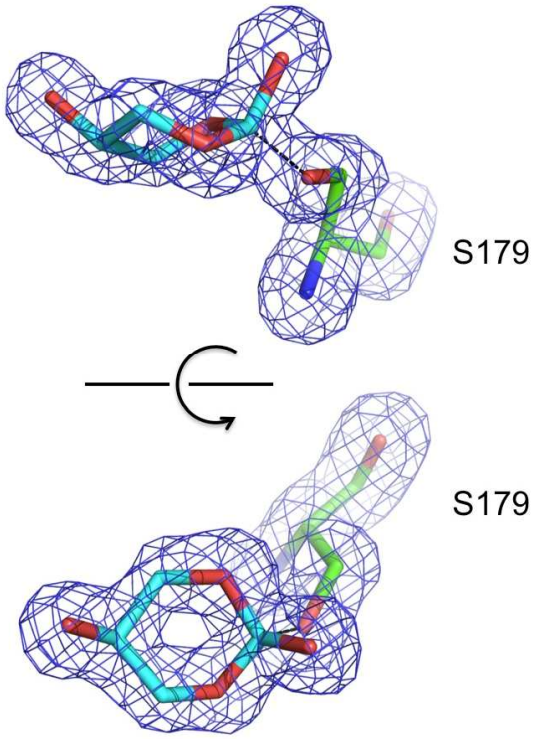

Figure 4

Highlights

• The crystal structure of hydrazidase complexed with a substrate is determined.

• A catalytic triad of Ser-cisSer-Lys in hydrazidase is revealed.

• His336 in a non-conserved region is a determinant for substrate specificity.